Tomography problems arising in Synthetic Aperture Radar

Cheney, Margaret

2000

CODEN:LUTEDX/(TEAT-7090)/1-16/(2000)

Tomography problems arising in Synthetic Aperture Radar

Margaret Cheney

Electromagnetic Theory
Department of Electrical and Information Technology
Lund University
Sweden

Margaret Cheney

Department of Mathematical Sciences
Rensselaer Polytechnic Institute
Troy, NY 12180
chenem@rpi.edu

Editor: Gerhard Kristensson

Abstract

This paper gives a mathematical tutorial on Synthetic Aperture Radar (SAR). We see that with the usual mathematical model, the SAR reconstruction problem reduces to a problem in integral geometry. A number of mathematical problems are posed; the paper concludes with a short description of the basic idea underlying the algorithms used in most present systems. The challenge to the mathematical community is to find algorithms that might be better.

1 Introduction and Mathematical Model

In the last forty years the engineering community has developed very successful microwave systems for making high-resolution images of the earth from airplanes and satellites. Such systems, which go under the general name Synthetic Aperture Radar (SAR), have received little attention in the mathematical community. The purpose of this paper is to give a tutorial on SAR and to point out some of the associated interesting and challenging mathematical questions.

In strip-mode Synthetic Aperture Radar (SAR) imaging, an antenna (on a plane or satellite) flies along a nominally straight track, which we will assume is along the x_2 axis. The antenna emits pulses of electromagnetic radiation in a more-or-less directed beam perpendicular to the flight track (i.e., in the x_1 direction). These waves scatter off the terrain, and the scattered waves are detected with the same antenna. The received signals are then used to produce an image of the terrain. (See Figure 1.)

The data depend on two variables, namely time and position along the x_2 axis, so we expect to be able to reconstruct a function of two variables.

1.1 The (simplified) partial differential equation

The correct model for radar is of course Maxwell's equations, but the simpler scalar wave equation is commonly used:

$$\left(\nabla^2 - \frac{1}{c^2(x)}\partial_t^2\right) U(t,x) = 0. \tag{1.1}$$

This is the equation satisfied by each component of the electric and magnetic fields in free space, and is thus a good model for the wave propagation in dry air. When the electromagnetic waves interact with the ground, their polarization is certainly affected, but if the SAR system does not measure this polarization, then (1.1) is an adequate model.

We assume that the earth is roughly situated at the plane $x_3 = 0$, and that for $x_3 > 0$, the wave speed is $c(x) = c_0$, the speed of light in vacuum (a good approximation for dry air).

The fundamental solution of the free-space wave equation [19] is $G_0(t-\tau, x-y)$, given by

$$G_0(t-\tau, x-y) = \frac{\delta(t-\tau-|x-y|/c_0)}{4\pi|x-y|}. \tag{1.2}$$

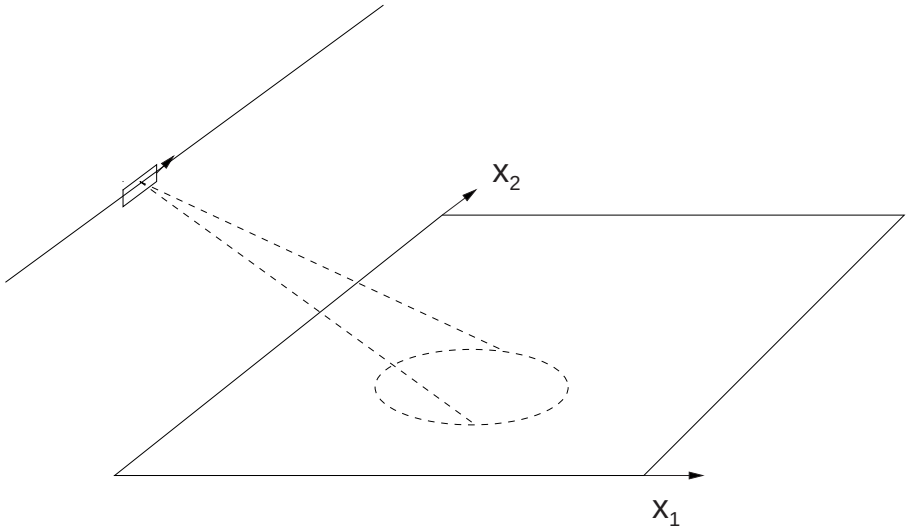

Figure 1: This shows the geometry of a conventional strip-mode SAR system.

It has the physical interpretation of the field at (x,t) due to a delta function point source at position y and time τ. This field satisfies the equation

$$\left(\nabla^2 - \frac{1}{c_0^2}\partial_t^2\right) G_0(t-\tau, x-y) = \delta(t-\tau)\delta(x-y). \tag{1.3}$$

1.2 The incident wave

The signal sent to the antenna is of the form

$$P(t) = A(t)e^{i\omega_0 t}, \tag{1.4}$$

where ω_0 is the (angular) *carrier frequency* and A is a slowly varying amplitude that is allowed to be complex.

If the source at y has the time history (1.4), then the resulting field $U_y(t, z-y)$ satisfies the equation

$$\left(\nabla^2 - \frac{1}{c_0^2}\partial_t^2\right) U_y(t, z-y) = P(t)\delta(z-y) \tag{1.5}$$

and is thus given by

$$\begin{aligned} U_y(t,z) = (G_0 * P)(t, z-y) &= \int \frac{\delta(t-\tau-|z-y|/c_0)}{4\pi|z-y|} P(\tau)d\tau \\ &= \frac{P(t-|z-y|/c_0)}{4\pi|z-y|} \\ &= \frac{A(t-|z-y|/c_0)}{4\pi|z-y|} e^{i\omega_0(t-|z-y|/c_0)}. \end{aligned} \tag{1.6}$$

The antenna, however, is not a point source. Most conventional SAR antennas are either slotted waveguides [8, 25] or microstrip antennas [18], and in either case, a good mathematical model is a rectangular distribution of point sources. We denote the length and width of the antenna by L and D, respectively. We denote the center of the antenna by x; thus a point on the antenna can be written $y = x + q$, where q is a vector from the center of the antenna to a point on the antenna. We also introduce coordinates on the antenna: $q = s_1\hat{e}_1 + s_2\hat{e}_2$, where $\hat{e}_1$ and $\hat{e}_2$ are unit vectors along the width and length of the antenna, respectively. The vector $\hat{e}_2$ points along direction of flight; for the straight flight track shown in Figure 1, this would be the x_2 axis. For side-looking systems as shown in Figure 1, $\hat{e}_1$ is tilted with respect to the x_1 axis so that a vector perpendicular to the antenna points to the side of the flight track.

We consider points z that are far from the antenna; for such points, for which $|q| << |z - x|$, we have the approximation

$$|z - y| = |z - x| - \widehat{(z - x)} \cdot q + O(L^2/|z - x|), \tag{1.7}$$

where the hat denotes a unit vector. We use this expansion in (1.6):

$$U_y(t, z) \sim \frac{A(t - |z - x|/c_0 + \widehat{z - x} \cdot q/c_0 + \cdots)}{4\pi|z - x|} e^{i\omega_0(t - |z-x|/c_0)} e^{ik\widehat{z-x}\cdot q} \tag{1.8}$$

where we have written $k = \omega_0/c_0$. This expansion is valid because we also have $kL^2 << |z - x|$. We now make use of the fact that $|z - x| >> \widehat{z - x} \cdot q$ and that A is assumed to be slowly varying to write

$$U_y(t, z) \sim \frac{P(t - |z - x|/c_0)}{4\pi|z - x|} e^{ik\widehat{z-x}\cdot q}. \tag{1.9}$$

Far from the antenna, the field from the antenna is

$$\begin{aligned} U_x^{in}(t, z) &= \int_{-L/2}^{L/2}\int_{-D/2}^{D/2} U_{x+s_1\hat{e}_1+s_2\hat{e}_2}(t, z)ds_1ds_2 \\ &\sim \int_{-L/2}^{L/2}\int_{-D/2}^{D/2} \frac{P(t - |z - x|/c_0)}{4\pi|z - x|} e^{ik\widehat{z-x}\cdot(s_1\hat{e}_1+s_2\hat{e}_2)}ds_1ds_2 \\ &\sim \frac{P(t - |z - x|/c_0)}{4\pi|z - x|} \int_{-L/2}^{L/2} e^{iks_2\widehat{z-x}\cdot\hat{e}_2}ds_2 \int_{-D/2}^{D/2} e^{iks_1\widehat{z-x}\cdot\hat{e}_1}ds_1 \\ &\sim \frac{P(t - |z - x|/c_0)}{4\pi|z - x|} w(\widehat{z - x}), \end{aligned} \tag{1.10}$$

where

$$w(\widehat{z - x}) = 2D\text{sinc}(k\widehat{z - x} \cdot e_1 D/2)\ 2L\text{sinc}(k\widehat{z - x} \cdot e_2 L/2) \tag{1.11}$$

is the antenna beam pattern and where $\text{sinc}\,\beta = (\sin\beta)/\beta$. The sinc function has its main peak at $\beta = 0$ and its first zero at $\beta = \pi$; this value of β gives half the width

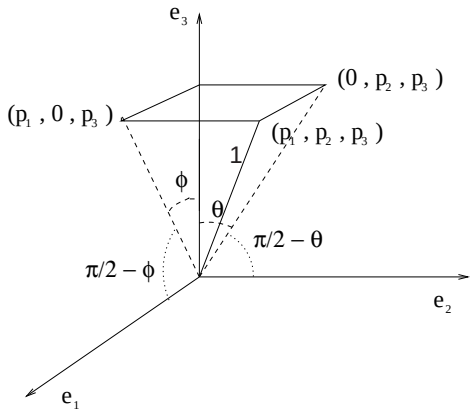

Figure 2: This is a diagram that shows that if $p = \widehat{z-x}$ is a unit vector, then $\hat{p} \cdot \hat{e}_2 = p_2 \approx \sin\theta$ and $\hat{p} \cdot \hat{e}_1 = p_1 \approx \sin\phi$. The antenna lies on the x_1-x_2 plane.

of the main peak. Thus the main beam of the antenna is directed in the direction perpendicular to the antenna.

We determine the width of the beam by noting that the first zero of $\text{sinc}(k\widehat{z-x} \cdot e_2 L/2)$ occurs when $k\widehat{z-x} \cdot \hat{e}_2 L/2 = \pi$. Using the fact that $2\pi/k$ is precisely the wavelength λ, we can write this as $\widehat{z-x} \cdot \hat{e}_2 = \lambda/L$. To understand this condition, we write $\widehat{z-x} \cdot \hat{e}_2 \approx \cos(\pi/2 - \theta) = \sin\theta \approx \theta$, an approximation that is valid for small angles θ. (See Figure 2.) Here θ is the angle between the vector normal to the antenna and the projection of $\widehat{z-x}$ on the plane spanned by $\hat{e}_2$ and $\hat{e}_3$. Thus when $\lambda << L$ and thus θ is small, the condition $\widehat{z-x} \cdot \hat{e}_2 = \lambda/L$ reduces to $\theta \approx \lambda/L$. In this case, the main lobe of the antenna beam pattern has angular width $2\lambda/L$ in the $\hat{e}_2$ direction. Similarly the angular width in the $\hat{e}_1$ direction is $2\lambda/D$. We note that smaller wavelengths and larger antennas correspond to more tightly focused beams.

The antenna beam pattern is not always precisely a product of sinc functions: the signal emanating from different parts of the antenna can be weighted so that the integrals appearing in (1.10) are Fourier transforms of functions smoother than characteristic functions [17]. Such weighting suppresses the sidelobes at the expense of broadening the main beam slightly.

The Swedish CARABAS system [13, 21, 22] uses two parallel wire antennas of length L that are oriented along the flight track. Each antenna can be considered a linear distribution of point sources, so the beam pattern of each antenna is

$$w_C(\widehat{z-x}) = 2L\text{sinc}(k\widehat{z-x} \cdot e_2 L/2) \tag{1.12}$$

The length L is chosen to be half the wavelength of the carrier wave (i.e., $kL/2 = \pi$), so that the antenna produces only one single main lobe.

1.3 A linearized scattering model

From classical scattering theory we know that a scattering solution of (1.1) can be written

$$\Psi(t,x) = \Psi^{in}(t,x) + \Psi^{sc}(t,x), \tag{1.13}$$

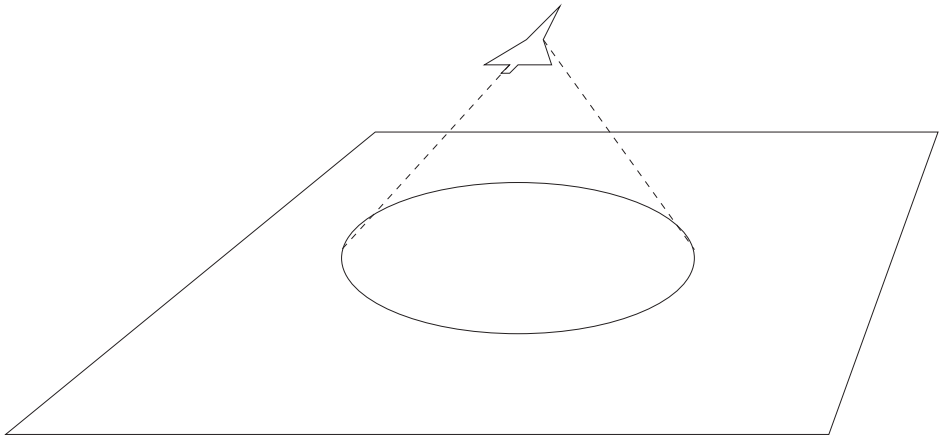

Figure 3: The geometry of the CARABAS SAR system.

where Ψ^{in} satisfies (1.1) with $c(x) = c_0$ and where (see Appendix)

$$\Psi^{sc}(t,x) = \int\int G_0(t-\tau, x-z)V(z)\partial_\tau^2\Psi(\tau,z)d\tau dz \tag{1.14}$$

and

$$V(z) = \frac{1}{c^2(z)} - \frac{1}{c_0^2}. \tag{1.15}$$

For commonly used carrier frequencies ω_0, the waves decay rapidly as they penetrate into the earth. Thus the support of V can be taken to be a thin layer at the earth's surface. This is discussed in more detail in section 3.

A commonly used approximation, often called the *Born approximation* or the *single scattering approximation*, is

$$\begin{aligned}\Psi^{sc}(t,x) \approx \Psi^B(t,x) &= \int\int G_0(t-\tau, x-z)V(z)\partial_\tau^2\Psi^{in}(t,x)d\tau dz \\ &= \int \frac{V(z)}{4\pi|x-z|}\partial_t^2\Psi^{in}(t-|x-z|/c_0, z)dz. \end{aligned}\tag{1.16}$$

The value of this approximation is that it removes the nonlinearity in the inverse problem: it replaces the product of two unknowns (V and Ψ) by a single unknown (V) multiplied by the known incident field.

The Born approximation makes the problem simpler, but it is not necessarily a good approximation. This issue is discussed briefly in section 3.2. Another linearizing approximation that can be used at this point is the *Kirchhoff approximation*, in which the scattered field is replaced by its geometrical optics approximation [14]. Here, however, we consider only the Born approximation.

In the case of SAR, the antenna emits a series of fields of the form (1.10) as it moves along the flight track. In particular, we assume that the antenna is located at position x^n at time nT, and there emits a field of the form (1.10). In other words, the incident field is

$$\Psi^{in}(\tau,z) = \sum_n \Psi_n^{in}(\tau,z), \tag{1.17}$$

where

$$\Psi_n^{in}(\tau, z) \sim \frac{P(\tau - nT - |z - x^n|/c_0)}{4\pi|z - x^n|} w(\widehat{z - x^n}) \tag{1.18}$$

is the nth emission. We use this expression in (1.16) to find an approximation to the scattered field due to the nth emission. The resulting expression involves two time derivatives of $P(t, x)$. In calculating these time derivatives, we use the fact that A is assumed to be slowly varying to obtain

$$\partial_t^2 P(t, x) \approx -\omega_0^2 P(t, x). \tag{1.19}$$

Thus the Born approximation to the scattered field due to the nth emission, measured at the center of the antenna, is

$$\begin{aligned} S_n(t) &\approx \Psi_n^B(t - nT, x^n) \\ &\approx -\int \frac{\omega_0^2 P(t - nT - 2|z - x^n|/c_0)}{4\pi|z - x^n|} \frac{V(z)}{4\pi|z - x^n|} w(\widehat{z - x^n}) dz. \end{aligned} \tag{1.20}$$

In (1.20), we note that $2|z - x^n|/c_0$ is the two-way travel time from the center of the antenna to the point z. The factors $4\pi|z - x^n|$ in the denominator correspond to the geometrical spreading of the spherical wave emanating from the antenna and from the point z.

In practice, the received signal is not measured at a single point in the center of the antenna; rather, the signal is received on the entire antenna. This means that the received signal is subject to the same weighting as the transmitted signal. Thus w in (1.20) should be replaced by w^2. We continue to write simply w.

2 Reduction to a delta function impulse

The SAR reconstruction problem would be a problem in integral geometry if the transmitted signal P were a delta function. Unfortunately, a delta function cannot be produced in practice. Nor can an approximate delta function be used: any short-time, limited-amplitude wave will contain little energy, and the reflected wave contains even less energy. A very low-energy wave will get drowned out by noise.

To circumvent this difficulty, SAR systems use *pulse modulation*, in which the system transmits a complex waveform and then *compresses* the received signal mathematically, to synthesize the response from a short pulse. This processing is explained in this section. The final result is that to a good approximation, P can indeed be replaced by a delta function.

2.1 Matched filter processing

The mathematical processing is done by applying a *matched filter* [20]. Applying a matched filter to the received signal means integrating it against a shifted copy of the complex conjugate of the transmitted signal:

$$O(t', x^n) = \int \overline{P(t - t')} S_n(t) dt$$

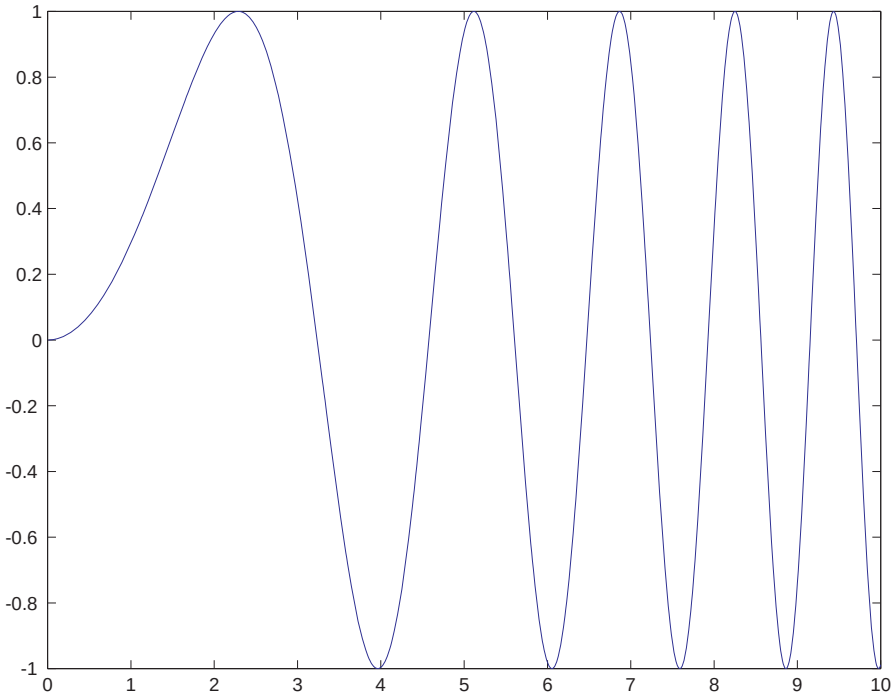

Figure 4: The chirp $\sin(.3t^2)$.

$$\begin{aligned} &\approx -\int \overline{P(t-t')} \int \frac{\omega_0^2 P(t-nT-2|z-x^n|/c_0)}{(4\pi|z-x^n|)^2} V(z) w(\widehat{z-x^n}) dz dt \\ &\approx \int \frac{\omega_0^2 \zeta(nT+2|z-x^n|/c_0-t')}{(4\pi|z-x^n|)^2} V(z) w(\widehat{z-x^n}) dz. \end{aligned} \tag{2.1}$$

where

$$\zeta(s-t') = \int \overline{P(t-t')} P(t-s) dt = \int \overline{P(s')} P(s'-(s-t')) ds' \tag{2.2}$$

is the *range ambiguity function* [10]. We see that matched-filter processing has the effect of replacing the waveform P in (1.20) by the *compressed* waveform ζ.

To determine ζ, we use (1.4):

$$\zeta(s) = \int \overline{A(t)e^{i\omega_0 t}} A(t-s) e^{i\omega_0(t-s)} dt; \tag{2.3}$$

we see that ζ is a complex number of modulus one multiplied by the autocorrelation function of A.

The modulation A should be chosen so that ζ is close to a delta function.

The most commonly used modulated pulse is a *chirp*, which involves linear frequency modulation. The idea is to label different parts of the wave by their frequency, and then superimpose these different parts in the compression process.

2.2 Instantaneous frequency

The notion of *instantaneous frequency* of a wave $F(t) = e^{i\phi(t)}$ derives from a stationary phase analysis of the usual Fourier transform integral: we think of the integrand of the Fourier integral

$$f(\omega) = \int F(t)e^{-i\omega t}dt = \int e^{i(\phi(t)-\omega t)}dt \tag{2.4}$$

as being written in the form $\exp(i\lambda(\phi(t) - \omega t))$, where $\lambda = 1$. The usual large-λ stationary phase calculation shows that the leading order contribution comes from the values of t at which the phase is not changing rapidly with respect to t. This occurs when $0 = (d/dt)(\phi(t) - \omega t)$, or in other words, when $\omega = d\phi/dt$. Thus we call $d\phi/dt$ the *instantaneous frequency* of F.

2.3 Chirps

A *chirp* is a finite wavetrain $P(t) = \chi_{[-\tau/2,\tau/2]}(t)\exp(i\phi(t))$ in which the instantaneous frequency changes linearly with time. Here $\chi_{[-\tau/2,\tau/2]}$ denotes the characteristic function of the time interval $[-\tau/2, \tau/2]$, which is one in this time interval and zero outside. In an *upchirp*, the instantaneous frequency increases linearly with time as $d\phi/dt = \omega_0 + Bt/\tau$, where ω_0 is the (angular) carrier frequency and B is called the (angular) *bandwidth*. To determine ϕ, we simply integrate to obtain $\phi(t) = \omega_0 t + Bt^2/(2\tau)$. Thus an upchirp is a wavetrain of the form

$$P(t) = \chi_{[-\tau/2,\tau/2]}(t)e^{i\alpha t^2}e^{i\omega_0 t}, \tag{2.5}$$

where $\alpha = B/(2\tau)$. We note that such a pulse is of the form (1.4), where

$$A(t) = \chi_{[-\tau/2,\tau/2]}(t)e^{i\alpha t^2}. \tag{2.6}$$

2.4 The compressed waveform ζ for a chirp.

For a chirp, ζ is

$$\begin{aligned} \zeta(s) &= e^{-i\omega_0 s}\int \overline{A(t)}A(t-s)dt & (2.7)\\ &= e^{-i\omega_0 s}\int \overline{\chi_{[-\tau/2,\tau/2]}(t)e^{i\alpha t^2}}\chi_{[-\tau/2,\tau/2]}(t-s)e^{i\alpha(t-s)^2}dt. & (2.8)\end{aligned}$$

After calculating the integral on the right side of (2.8), we obtain

$$\zeta(s) = e^{-i\omega_0 s}e^{iBs^2/(2\tau)}\frac{2\tau\sin(Bs(1-|s|/\tau)/2)}{Bs}\chi_{[-\tau,\tau]}(s) \tag{2.9}$$

By taking B sufficiently large, we can make ζ peak arbitrarily sharply at zero.

Other modulated waveforms besides chirps can also be used to obtain a range ambiguity function ζ that approximates a delta function.

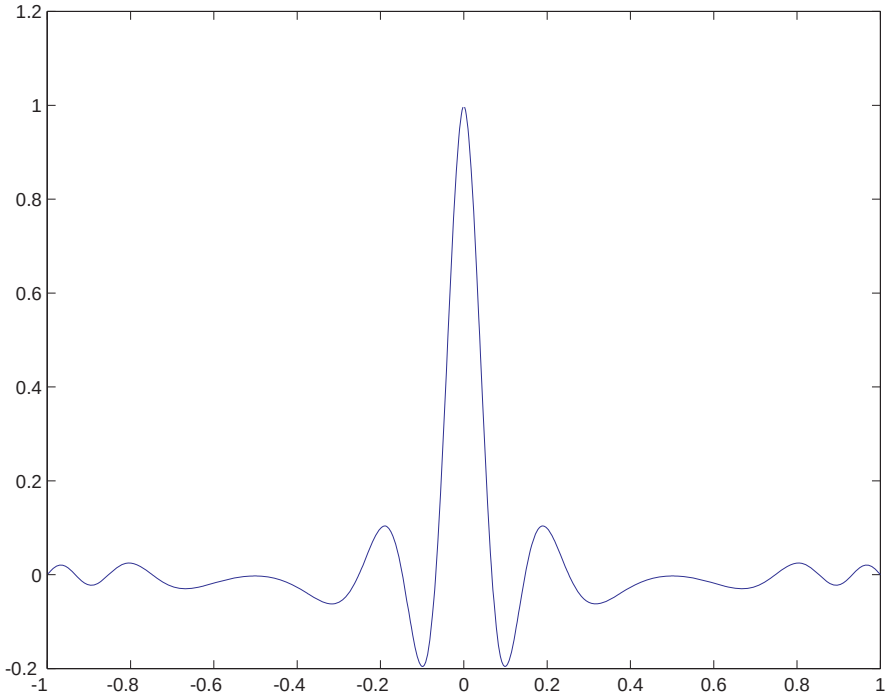

Figure 5: The amplitude of the function ζ for $\tau = 1$ and $B = 100$.

3 Mathematical Problems

If we replace ζ in (2.1) by a delta function, then (2.1) becomes

$$O_{\mathrm{C}}(t', x^n) = \frac{\omega_0^2}{(2\pi^2 c_0(t' - nT))^2} \int \delta((nT - t') - 2|z - x^n|/c_0) V(z) w(\widehat{z - x^n}) dz \quad (3.1)$$

We see that the radar reconstruction problem becomes a problem in integral geometry: reconstruct $V(z)$ from its weighted integrals over the spheres $|z - x^n| = c_0(nT - t')/2$. Here $x^n = x(nT)$, where $x(s)$ is a known path (flight track) in space. This problem requires some discussion.

In (3.1), for a straight flight track, O depends on two variables, namely time and position along the line, whereas V appears to depend on three variables. However, as mentioned earlier, V can be considered to have support in a thin layer at the surface. In the case in which the terrain is planar (a good approximation when the flight track is at satellite height), we can replace $V(z)$ by $V(z_1, z_2)\delta(z_3 - 0)$, where $V(z_1, z_2)$ is referred to as the *ground reflectivity function*. In this case (3.1) reduces to a two-dimensional integral.

For lower-altitude flight tracks, the ground topography becomes important. In this case, we replace $V(z)$ by $V(z_1, z_2)\delta(z_3 - h(z_1, z_2))$, where h is the ground altitude. In this case, the problem is to reconstruct two functions of two variables; generally one uses data from two parallel flight tracks.

Some key aspects of the reconstruction problem depend on the weighting function w: the CARABAS system, for example, has a symmetrical beam pattern (1.12), so

that from a single antenna moving along a straight line, it is not possible to determine whether a given reflection originated from a point to the left of the antenna or to the right. It is for this reason that the CARABAS system uses two antennas. Conventional side-looking SAR avoids this problem by using a focused beam (1.11) that is directed to one side of the flight track (see Figure 1).

To be of most practical use, reconstruction algorithms should be fast, accurate, and should use as little memory as possible. Ideally they should allow an image to be constructed in real time as the aircraft or satellite flies along the flight track. The amount of data collected by SAR systems can be enormous.

3.1 Integral geometry problems

We simplify the problem by making the change of variables $t = c_0(nT - t')/2$. Then for planar topography, the idealized SAR reconstruction problem is to reconstruct V from

$$\text{data}(t, x(s)) = c \int_{t=|z-x|} V(z_1, z_2)\delta(z_3)w(\widehat{z-x})dz \tag{3.2}$$

where c is a known constant, $x(s)$ is a known path above the plane $z_3 = 0$ and w is the known antenna beam pattern that depends only on the direction $\widehat{z-x}$. Because the spheres $t = |z - x|$ intersect the plane $z_3 = 0$ in circles, this problem is to reconstruct $V(z_1, z_2)$ from its weighted integrals over circles or circular arcs. Relevant references here are [2, 12, 13, 15, 21].

For non-planar topography, the idealized SAR reconstruction problem is to reconstruct both V and h from the integrals

$$\text{data}(t, x) = c \int_{t=|z-x|} V(z)\delta(z_3 - h(z_1, z_2))w(\widehat{z-x})dz, \tag{3.3}$$

where x lies on one or more flight tracks above the plane $z_3 = 0$. A relevant reference is [22].

Before making an attack on the full non-planar topography problem, a reasonable warm-up problem is to begin with the case $V = 1$, $w = 1$. This problem is to recover the surface height h from

$$\text{data}(t, x) = c \int_{t=|z-x|} \delta(z_3 - h(z_1, z_2))dz. \tag{3.4}$$

Probably at least two paths $x(s)$ are needed; a relevant reference is again [22].

In addition to the challenge of developing and analyzing reconstruction algorithms, some relevant questions are the following.

3.1.1 Problems related to the flight track

Generally the flight tracks are approximately straight lines. Are straight lines best? Here [2] is relevant. A robust reconstruction algorithm must be able to deal with flight tracks $x(t)$ that deviate from a straight line by known perturbations. Airplanes, in addition, are subject to turbulence in the atmosphere, which means that

they are subject to pitch, roll, and yaw. In terms of (1.11), this means that the orientation of the vectors e_1 and e_2 varies with time or with n. In terms of the idealized problem (3.2), this means that w depends on x as well as on the unit vector $\widehat{z-x}$. A book on SAR with a section about motion correction is [12].

Issues related to a non-ideal flight track become even more important in military applications, when enemy fire can induce the aircraft to take evasive action. Can we find a reconstruction algorithm that can use data from a wild flight track? In the study of this issue, [2] is relevant.

3.1.2 Breaking the left-right symmetry

How can a reconstruction algorithm best take advantage of the two antennas of the CARABAS system? In this case one can assume that the weighting function w is simply one, but that there are two parallel flight tracks. Presumably, if the antennas were moved closer together, it would become more difficult to determine whether a given reflection comes from the left or the right of the flight track. This should be quantified.

3.1.3 Resolution

For a given carrier frequency ω_0, antenna pattern w, and bandwidth B, what is the best resolution that can be achieved? Is the resolution improved by incorporating information from many flight tracks? Relevant references are [16] and [21].

3.2 Other mathematical problems

3.2.1 Scatterers that move

For moving objects such as trains on a railway, the Doppler effect combined with pulse compression techniques results in incorrect estimates for the location of the moving object. How can this be corrected?

For systems that use the correlation between many “looks" to form an image, smaller moving objects tend to disappear. How can these moving objects be imaged? Can their velocity be determined? A relevant reference is [23].

3.2.2 Improvement of the model

All the current processing is based on a linearizing assumption such as the Born approximation (1.16), which amounts to assuming that the wave scatters only once before returning to the antenna. But in many cases, this model is believed to be too simple. For example, in scanning a forest at low frequencies, the most important scattering mechanism is believed to be double scattering (see Figure 6) in which the wave reflects first from the ground and then from the tree trunk (or vice versa).

The mathematical difficulty is that including multiple scattering makes the inverse problem nonlinear. Can we develop reconstruction algorithms for the nonlinear case?

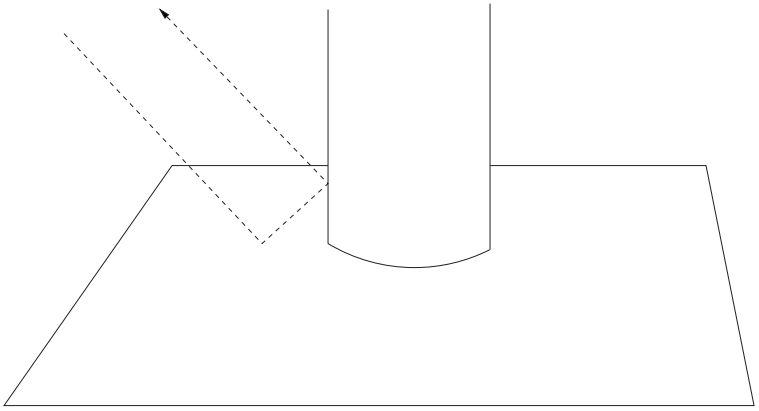

Figure 6: Double scattering from a tree trunk and ground.

The entire theory should be extended to the case of Maxwell's equations, for a model of *polarimetric SAR*.

3.2.3 Theoretical issues

Little is known about the nature of the inverse scattering problem for the wave equation in the case when only backscattering data is measured. Does backscattering data uniquely determine a scatterer?

4 How the Processing is Done Currently

Present SAR image reconstruction algorithms are based on the notion of matched filters: at each "look" (i.e., at each n), a matched filter is applied to the received signal $S_n(t)$:

$$I_n(y) = \int \overline{P(t - nT - 2|y - x^n|/c_0)} S_n(t) dt. \tag{4.1}$$

This correlates the received signal with a signal proportional to that due to a "point scatterer" at position y (i.e., take $V(z) = \delta(z - y)$ in the Born approximation).

If we use expression (1.20) (with $|z - x^n|$ replaced by R_0) in (4.1) and interchange the order of integration, we find

$$I_n(y) \approx \int W_n(y, z) \frac{-\omega_0^2 V(z)}{(4\pi R_0)^2} dz. \tag{4.2}$$

Here

$$W_n(y, z) = w(\widehat{z - x^n}) \int \overline{P(t - nT - 2|y - x^n|/c_0)} P(t - nT - 2|z - x^n|/c_0) dt \tag{4.3}$$

represents the *point spread function* of this single-look imaging system: if $V(z) = \delta(z - z_0)$, then $I_n(y) = W_n(y, z_0)$ would be proportional to the resulting image of V.

The key idea of SAR is that this point spread function can be made closer to a delta function by summing over n, i.e., by combining information from multiple looks. Thus the final image is formed as

$$I(y) = \sum_n I_n(y) \approx \int W(y,z) \frac{-\omega_0^2 V(z)}{(4\pi R_0)^2} dz, \tag{4.4}$$

with the point spread function

$$W(y,x) = \sum_n W_n(y,z) \tag{4.5}$$

This point spread function is called the *generalized ambiguity function* of the SAR system. By taking P to be a chirp or other modulated waveform, W becomes an approximate delta function. An analysis of W, which gives the resolution of the SAR system, can be found in [4, 6], and many other sources.

The matched filter reconstruction algorithm results in a complex-valued image. The phase of this image contains information about the distance of the scatterer from the antenna. To recover the ground topography, one uses a technique called *interferometric SAR* [3, 12], in which one uses the interference pattern from two complex images from parallel flight tracks.

Standard matched filter reconstruction algorithms cannot be used for the CARABAS system; instead a filtered backprojection scheme [15] is currently used.

5 Acknowledgments

I would like to thank Lars Ulander and Hans Hellsten for teaching me about the CARABAS system; many of the open problems listed here were suggested by them. I am also grateful to Ehud Heyman and Anders Derneryd for helpful discussions, and to Frank Natterer, Brett Borden, and Todd Quinto for reading the manuscript and making helpful suggestions regarding the exposition.

This work was partially supported by the Office of Naval Research, by Rensselaer Polytechnic Institute, by Lund University through the Lise Meitner Visiting Professorship, and by the Engineering Research Centers Program of the National Science Foundation under award number EEC-9986821.

Appendix A Classical scattering theory

To obtain (1.14), we first write $U = \Psi = \Psi^{in} + \Psi^{sc}$ in (1.1); this gives us

$$\left(\nabla^2 - c_0^{-2}\partial_t^2\right)\Psi^{sc} - V\partial_t^2\Psi = 0 \tag{A.1}$$

We then multiply (A.1) by G_0, multiply (1.3) by Ψ^{sc}, and subtract the resulting two equations to obtain

$$G_0\nabla^2\Psi^{sc} - \Psi^{sc}\nabla^2 G_0 - G_0 V\partial_t^2\Psi = G_0\Psi^{sc}\delta \tag{A.2}$$

We then integrate over all time and over a large ball, use Green's identity, and let the radius of the ball go to infinity. The integral involving the spatial derivatives vanishes, and we are left with (1.14).

We note that (1.14) shows that the notion of a a point scatterer is problematic. If we take $V(y) = \delta(y - y^0)$ in (1.14), we obtain

$$\Psi^{sc}(t,z) = \int G_0(t-\tau, z, y^0)\partial_\tau^2 \Psi(\tau, y^0) d\tau = \frac{\partial_t^2 \Psi(t - |z-y^0|/c_0, y^0)}{4\pi|z-y^0|}, \qquad \text{(A.3)}$$

which shows that the scattered field at the point y^0 is singular (unless $\partial_t^2 \Psi(t, y^0)$ is zero for all time). But the product of a delta function with a singular function has no conventional meaning. The issue of point scatterers has been studied in [1].

Note, however, that in the Born approximation, the field scattered from a point scatterer is well-defined and nonzero.

References

[1] S. Albeverio, F. Gesztesy, R. Høegh-Krohn, and H. Holden, Solvable Models in Quantum Mechanics, Texts and Monographs in Physics, Springer-Verlag, New York, 1988.

[2] M. Agranovsky and E.T. Quinto, Injectivity sets for the Radon transform over circles and complete systems of radial functions, J. Functional Analysis 139 (1996) 383–414.

[3] R. Bamler and P. Hartl, "Synthetic aperture radar interferometry", Inverse Problems 14 (1998) R1–R54.

[4] M. Cheney, "A mathematical tutorial on Synthetic Aperture Radar", to appear, SIAM Review.

[5] J.C. Curlander and R.N. McDonough, Synthetic Aperture Radar, Wiley, New York, 1991.

[6] L.J. Cutrona, "Synthetic Aperture Radar", in Radar Handbook, second edition, ed. M. Skolnik, McGraw-Hill, New York, 1990.

[7] H. T. Cuong, A. W. Troesch, T. G. Birdsall, "The Generation of Digital Random Time Histories", Ocean Engineering, 9 (1982) 581–588.

[8] A. Derneryd and A. Lagerstedt, "Novel slotted waveguide antenna with polarimetric capabilities", Proc. of IGARSS Conference, Firenze, Italy (1995) 2054–2056.

[9] A.G. Derneryd, R.N.O. Petersson, P. Ingvarson, "Slotted waveguide antennas for remote sensing satellites", Proceedings of PIERS conferences, Noordwijk, The Netherlands (July 1994).

[10] B. Edde, Radar: Principles, Technology, Applications, Prentice Hall, New York, 1993.

[11] C. Elachi, Spaceborne Radar Remote Sensing: Applications and Techniques, IEEE Press, New York, 1987.

[12] G. Franceschetti and R. Lanari, Synthetic Aperture Radar Processing, CRC Press, New York, 1999.

[13] H. Hellsten and L.E. Andersson, "An inverse method for the processing of synthetic aperture radar data", Inverse Problems 3 (1987), 111–124.

[14] K.J. Langenberg, M. Brandfass, K. Mayer, T. Kreutter, A. Brüll, P. Felinger, D. Huo, "Principles of microwave imaging and inverse scattering", EARSeL Advances in Remote Sensing, 2 (1993) 163–186.

[15] Stefan Nilsson, "Application of fast backprojection techniques for some inverse problems of integral geometry", Linköping Studies in Science and Technology, Dissertation No. 499 (1997).

[16] F. Natterer, The Mathematics of Computerized Tomography, Wiley, New York, 1986.

[17] A.V. Oppenheim and R.W. Shafer, Digital Signal Processing, Prentice-Hall, Englewood Cliffs, New Jersey, 1975.

[18] R.N.O. Petersson, A.G. Derneryd, and P. Ingvarson, "Microstrip antennas for remote sensing satellites", Proceedings of PIERS conferences, Noordwijk, The Netherlands (July 1994).

[19] F. Treves, Basic Linear Partial Differential Equations, Academic Press, New York, 1975.

[20] C.W. Therrien, Discrete Random Signals and Statistical Signal Processing, Prentice Hall, Englewood Cliffs, New Jersey, 1992.

[21] L. M. H. Ulander and H. Hellsten, "A new formula for SAR spatial resolution", AEÜ Int. J. Electron. Commun. 50 (1996) no. 2, 117–121.

[22] L.M.H. Ulander and P.-O. Frölund, "Ultra-wideband SAR interferometry", IEEE Trans. on Geoscience and Remote Sensing, vol. 36 no. 5, September 1998, 1540–1550.

[23] L.M.H. Ulander and H. Hellsten, "Low-frequency ultra-wideband array-antenna SAR for stationary and moving target imaging", conference proceedings for the SPIE 13th Annual International Symposium on Aerosense, Orlando, Florida, April 1999.

[24] L.J. Ziomek, Underwater Acoustics: A Linear Systems Theory Approach, Academic Press, Orlando, 1985.

[25] R. Zahn and M. Schlott, "Active antenna for X-band space SAR", Proc. Int. Conf. on Radar, Paris, France, (1994) 36–41.